Journal of Cluster Science (2020) 31:549–560
https://doi.org/10.1007/s10876-019-01673-x

ORIGINAL PAPER

Gold Nanoparticles Biosynthesized Using *Ginkgo biloba* Leaf Aqueous Extract for the Decolorization of Azo-Dyes and Fluorescent Detection of Cr(VI)

Ying Liu[1] · Liping Huang[1] · Sakil Mahmud[1,2,3] · Huihong Liu[1]

Received: 24 July 2019 / Published online: 11 September 2019

Abstract

Gold nanoparticles (AuNPs) are successfully synthesized via a facile and eco-friendly biosynthesis approach. *Ginkgo biloba* (*G. biloba*) leaf is an extract used as bio-aqueous solution for the preparation of the AuNPs. Photo-chemically, the *G. biloba* leaf plays dual roles wherein it serves as reducing and stabilizing agent. Through this approach, the use of toxin-induced chemical is completely avoided making the approach a green chemistry. Several synthetic parameters such as reactant concentration, media pH, reaction time and temperature are optimized which in turn enables the formation of AuNPs with uniform size. Various analytical techniques including scanning electron microscope (SEM), high resolution-transmission electron microscopic (HRTEM), X-ray diffraction (XRD), energy dispersive X-ray (EDX) spectroscopy, fringe spacing and selected area diffraction (SEAD) pattern, and dynamic light scattering (DLS) are used for AuNPs characterization. The AuNPs exhibit cubic structure and spherical shape with average size of 18.95 ± 5.95 nm. The homemade AuNPs show promises in the catalytic decolorization of azo-dyes in the presence of sodium borohydride ($NaBH_4$). In addition, the AuNPs show appreciable sensitivity for the detection of Cr(VI) with a detection limit found to be 0.1–0.8 μM. This study is expected to spur further works on the use of metal nanoparticle for environmental pollution remediation.

Keywords Gold nanoparticles · *Ginkgo biloba* leaf · Biosynthesis · Azo-dyes · Fluorescence · Chromium ion

Introduction

The use of bio-nanocomposite for water and environmental remediation have recently attracted significant attention. This is due to their unique advantages such as non-toxicity, easy fabrication and cost viability [1, 2]. In particular, plant extracts are capable of enhancing user-friendliness, eco-friendliness, cost viability and large production of the nanoparticles (NPs) relevant for metal ions detection and wastewater decolonization [3]. In the plant-mediated synthesis of NPs, phytochemicals like polyphenols, terpenoids [4] and biomolecules such as proteins, amino acids, vitamins, polysaccharides, have been widely employed as reducing and stabilizing agents [5–7]. Among the NPs, gold nanoparticles (AuNPs) has been proved to be a good material with high compatibility with different kind of plant extracts such as *Coriander leaf*, *Cinnamomum camphora*, *Eucommia ulmoides*, *Aloevera*, etc. This is due to the eco-friendly nature of the AuNPs [3, 8–11]. Therefore, *Ginkgo biloba* (*G. biloba*) leaf is attempted and chosen as a potential candidate for the biosynthesis of AuNPs.

In term of archeological view, *G. biloba*, was discovered on the earth in the past 200 million years [12]. It is only a living species of the plant in the Ginkgophyta division. They are relatively common, cheap and easy to obtain [12].

✉ Sakil Mahmud
sakilmahmud@nimte.ac.cn

✉ Huihong Liu
huihongliu@wtu.edu.cn

[1] Resource Regenerating Institute, School of Chemistry and Chemical Engineering, Wuhan Textile University, Wuhan 430200, People's Republic of China

[2] Ningbo Institute of Materials Technology and Engineering, Chinese Academy of Sciences, Ningbo 315201, Zhejiang, People's Republic of China

[3] University of Chinese Academy of Sciences, Beijing 100049, People's Republic of China

In countries like Korea, Japan, China, Europe, and the USA. *G. biloba* leaf is commonly used as in medicinal extract, and additives in food and cosmetics [13]. The chemical constituents of *G. biloba* leaf are organic acids, bioflavonoids, polyprenols, terpenolds [14]. In term of material synthesis, the extracts from *G. biloba* leaf have been used as a reducing and stabilizing agent for the synthesis of NPs such as silver [15], copper [16] and graphene [17]. It is worth noting that *G. biloba* leaf has previously used for the synthesize of AuNPs [18], the details about synthesis and applications, especially in the field of fluorescent sensing metal, have never been presented. Hence, synthetic parameter optimization relevant for the preparation of AuNPs from *G. biloba* leaf worth investigation. Furthermore, when the menace of water and environmental pollution is being considered, the use of such cheap, cost-saving and biosynthesized AuNPs for water remediation needs to be investigated.

For instance, chromium is the heavy metal that has been extensively used in a wide range of manufacturing procedures [19, 20]. This has resulted in an enormous amount of toxic Cr [especially Cr(VI)] in the environment. Cr(VI) is the second most ample inorganic element in term of groundwater pollutants [21]. This has caused a lot of threats to human health and environment [19]. Due to the extreme toxicity of the Cr(VI) even at low concentration, the threshold limit has been set by governments of many countries [20, 22]. Due to this regulation, various approaches have been designed for the simultaneous detection and quantification of Cr(VI) in the different water chemistries [23–29]. The efficiency of these methods are often hampered by their complexity and long sample pretreatment routes. These have limited their practical application for the quick detection of Cr(VI) ions. Hence, it is necessary to develop a reliable analytical method which is capable of rapid detection of Cr(VI) while giving selectivity a consideration. Herein, an eco-friendly method is reported for efficient and rapid detection of Cr(VI) on the surface of AuNPs.

In addition to the above, dyes are known to be major environmental pollutants released into the environment by textiles, cosmetics, food, leather, and plastic industries [30]. Most of these dyes and associated toxic chemicals (e.g. formaldehyde, hydrocarbons, anthraquinone, nitro- and chloro-group, etc.) are non-biodegradable. As such, they endanger the life of aquatic species upon their release into water bodies [31]. Not only the aquatic life, but they also have tendencies to cause cancer and cell mutation in the human system [32]. So far, many methods have been designed for the removal and degradation of these dyes in aqueous solutions. Examples of such methods are photoelectric degradation [33], adsorption [34], microwave-assisted degradation [35], and photocatalytic reduction [36, 37]. However, most of these approaches are somehow time and energy-consuming. Based on this view, simple and fast methods wherein bio-green NPs are used is urgently need for efficient removal of hazardous dyes from every kind of water chemistries.

In this study, a simple and green biosynthetic method is used to prepare and control the size and shape of AuNPs. The influence of various synthetic parameters (e.g. mixing ratio of the reactants, reaction duration, temperature and pH of medium) are explored. Moreover, the potential applications of the as-synthesized AuNPs as catalytic degradation of azo-dyes in the presence of sodium borohydride (i.e. electron sacrificer) and the fluorescent probe for the determination of Cr(VI), are assessed.

Materials and Methods

Materials

Sodium hydroxide (NaOH), sodium borohydride ($NaBH_4$), and chloroauric acid ($HAuCl_4$) were analytical grade and supplied by Sinopharm Chemical Reagent Co., Ltd., Shanghai, China. Reactive yellow 179 (RY179) and Reactive yellow 145 (RY145) are the azo dyes purchased from DyStar Colours Deutschland GmbH, Germany. The Cr(VI) standard solution (prepared from $K_2Cr_2O_7$) was purchased from Chinese Standard Reference Materials Center, Beijing, China. All aqueous solutions are prepared using deionized water produced by a Labpure Water System (Chengdu, China).

Preparation of Leaf Extracts

The *G. biloba* leaf were sampled from the garden of Wuhan Textile University, Wuhan, China. The aqueous extract of *G. biloba* leaf was produced by mixing 5.0 g of the bark powder into 100 mL of deionized water. It is incubated in a water bath at 80 °C for 1 h. The extracts were then filtered to eliminate particulate substance and to get clear solutions which were then stored at refrigerator (4 °C) for subsequent experiments.

Biosynthesis of Green AuNPs

The *G. biloba* leaf aqueous extract was mixed into the aqueous solution (0.5 mM) of $HAuCl_4$ in 10 mL flask. The entire volume of the reactant was 5 mL. The sealed flask incubated in the water bath for several minutes at a constant temperature after configuring the concentration of reactants and solution pH. The colloidal solution was conditioned to the room temperature and stored properly for relevant characterizations.

Characterizations

Initial characterization of the AuNPs was conducted using UV–vis spectrophotometer (Tu-1901, Purkinje General Instrument Co. Ltd, Beijing, China) with wavelength ranging from 200 to 800 nm. A scanning electron microscope (SEM, JEOL 6460LV, Tokyo, Japan) was used to capture the morphology. Inca automate and mapping software was used to quantify the data collection and image processing. The high-resolution transmission electron microscopy (HRTEM, JEOL-JEM-2100F, Tokyo, Japan) was used to visualize the morphology of the AuNPs. HRTEM was also used to study the fringe spacing and selected area diffraction (SEAD) pattern. TEM deployed energy dispersive X-ray spectrometer (EDX, JSM-7600F) signal was also recorded to confirm the existence of metallic Au. The particle size range of the AuNPs along with its polydispersity was estimated using a particle size analyzer (ZEN 3600 Zetasizer, Malvern, England). Particle size was arrived based on measuring the time-dependent fluctuation of scattering of laser light by the NPs undergoing Brownian motion. X-ray diffraction (XRD) analysis was performed out using a Bruker AXS D8 Advance X-ray diffractometer. Fluorescence spectra were recorded by operating the F-2500 spectrophotometer (Hitachi, Japan).

Catalytic Decolorization of Azo Dyes

In order to assess the catalytic activity of as-synthesized AuNPs, 100 μL $NaBH_4$ (0.2 M) were added into 3 mL of the azo-dye solution (30 mg/L) in a 10 mL plastic tube, then 30 mL AuNPs were added in the plastic tube. After stirring thoroughly, the mixture was immediately transferred into a quartz cell. The UV–Vis spectra of the solution were collected at room temperature in a range of 200–700 nm using a quartz cell (1 cm path length). Therefore, the change of absorbance was used as a criterion to assess the reduction capability.

Fluorescent Sensing Cr(VI)

The fluorescence sensing experimentations of as as-synthesized AuNPs toward Cr(VI) were typically tested in Phosphate buffered saline (PBS) buffer that was used to configure pH at 9.0. Different concentrations of Cr(VI) solution was added and stirred carefully, and then the mixture was left to equilibrate for 15 min at room temperature before determination. The fluorescence quenching spectra were documented with excitation at 308 nm.

Results and Discussion

Biosynthesis of AuNPs

During the biosynthesis of the AuNPs, a gradual change in the color of the colloidal solution is observed. Typically, there is a formation of the colorful colloidal solution immediately after the addition of the *G. biloba* leaf extract into $HAuCl_4$ solution. This indicates the formation of AuNPs colloidal solution (Fig. 1 inset). However, a gradual change in the color from pale pink to purple-red is observed. The rate at which the color changes depends on the various parameters which include reactants mixing ratio, solution pH, reaction temperature and duration. The successful synthesis of AuNPs was confirmed by using UV–vis spectroscopy wherein light absorption spectra were taken. A typical plasmon resonance is found to be 530 nm which belongs to AuNPs (Fig. 1c) which ensure a successful formation of nanoparticles. Furthermore, pure *G. biloba* leaf extract (Fig. 1a) and $HAuCl_4$ solution (Fig. 1b) are used as reference samples, and their light absorption spectra are taken for comparison.

It is established that the *G. biloba* leaf extract comprises amide and polyphenols [38]. The reducing capabilities of antioxidant phytochemicals of *G. biloba* particularly polyphenolics may act as a primary reducing and polar agents [17]. Therefore, the reduction mechanism of AuNPs by quercetin 3-*O*-α-L-(β-D-glucopyranosyl)-(1,2)-rhamnopyranoside as one of the major antioxidants is shown in Scheme 1. Obviously, the influences of other phytochemicals are also responsible. However, the hydroxyl (–OH) group of phytochemicals is oxidized, Au ion being reduced to AuNPs. The composition contained in the extract may capped the particle surface by creating a thin

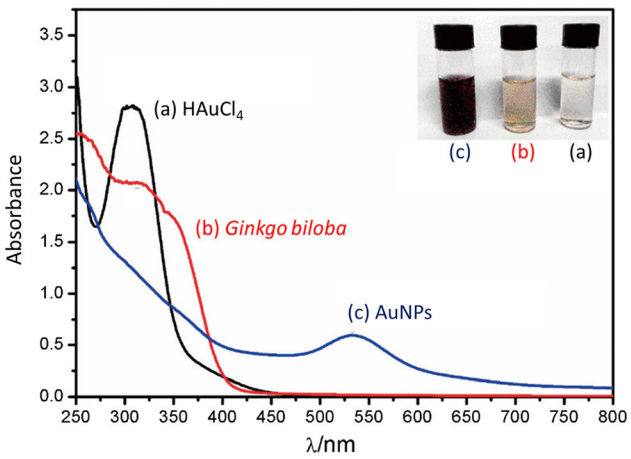

Fig. 1 UV–vis spectra of (a) *G. biloba* leaf aqueous extract, (b) $HAuCl_4$, (c) the as-synthesized AuNPs and their corresponding physical appearance in the inset

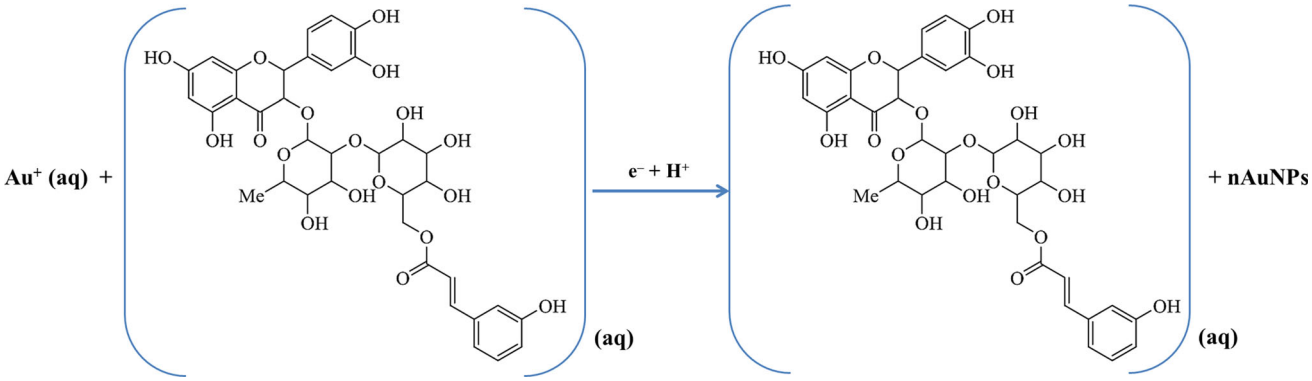

Scheme 1 Reduction mechanism of AuNPs by the extract of *G. Biloba* leaf

layer of cladding, thus prevent the individual particles from aggregation.

Optimization of AuNPs

It is well known that the surface plasmonic resonance (SPR) bands are oftentimes influenced various factors which include the shape, size, morphology, composition and dielectric environment of the NPs [39]. Moreover, the broadness of the SPR band can be related to good distribution of AuNPs and its active sites. As such, synthetic parameters i.e. reactants mixing ratio, pH of the solution, reaction temperature and incubation time that have a direct influence on the shape and size distribution of AuNPs [10, 40], are investigated. With this, biosynthetic parameters relevant to the fabrication of AuNPs with small sizes and uniform distribution are optimized.

Figure 2a reveals the absorption spectra of as-synthesized AuNPs using various concentrations of *G. biloba* leaf extract at a fixed concentration (0.5 mM) of $HAuCl_4$. As shown in Fig. 2a, when 0.5 mL of the *G. biloba* leaf extract is used, the maximum wavelength (λ_{max}) is found at 530 nm with absorbance = $\sim$ 0.586. Further increase in the concentration of *G. biloba* leaf extract shows only marginal differences in the position of λ_{max}. Therein, the addition of 1 mL, 1.5 mL, 2 mL, and 2.5 mL changes the λ_{max} to 541 nm, 568 nm, 601 nm and 617 nm respectively. This shows that *G. biloba* leaf extract is a good stabilizing agent, and its concentration is invariant with the size of the AuNPs. Therefore, 0.5 mL of the *G. biloba* leaf extract as an optimized amount is selected for further experiments.

Temperature is another crucial factor that influences the formation of AuNPs [10, 41]. In order to investigate the effect of temperature on the size and active site distribution of the AuNPs, the temperature is varied from 40 to 90 °C (Fig. 2b). It is found out that the SPR bands at 548 nm, 541 nm, and 530 nm correspond to the synthetic temperature of 40 °C, and 50 °C, respectively. However, when the temperature further increases to 60 °C, 70 °C, 80 °C, and 90 °C, the position of the SPR band reduces to 530 nm. In fact, it is observed that at higher synthetic temperature (> 50 °C), the SPR bands appear at the same at λ_{max}. This may be due to particle aggregation and increase in particle sizes which reduces the active site exposure. Hence, the temperature of 60 °C is considered as the optimum temperature for the preparation of AuNPs via the biosynthetic method.

It has been proved that the sizes of AuNPs can be influenced by the pH of the solution [42, 43]. Figure 2c proves the effect of pH on the synthesis of AuNPs. By increasing solution pH from 4 to 10, the SPR bands exhibit a blue shifted from 527 nm at pH 4 to 530 nm at pH 10. Moreover, a further increase in the pH to 12 gives rise to more blue shift wherein the absorption peak is found at 541 nm whereas the absorbance decreases with increase in the solution pH. This shows that solution pH exerts influence on particle aggregation and the formation rate of the NPs. Therefore, pH 10 is selected as the optimum pH for the synthesis of AuNPs in the experiments.

Accurate reaction time is essential for the entire nucleation and stability of AuNPs [10, 44]. The UV–vis absorption spectra of the as-synthesized AuNPs as a function of different reaction time between its precursors are shown in Fig. 2d. The spectra show the λ_{max} at 530 nm which increases progressively with increase in the reaction time. This specifies continuous reduction of the Ag ions and increases in the formation amount of the AuNPs. The broadness of the SPR peak is seen decreasing with reaction time. This indicates that a uniform distribution of AuNPs with narrow size. Further increase in the reaction time (> 30 min) shows no significant effect on the absorbance. Hence, the reaction time of 30 min is selected as the optimum duration.

The condition of the environment (i.e. seasons) has greatly influenced the phytochemicals in *G. biloba* leaf [14, 45]. Figure 3 exhibits the synthesis of AuNPs at optimized condition using the aqueous extracts from *G. biloba* leaf sampled in different months of the year. The

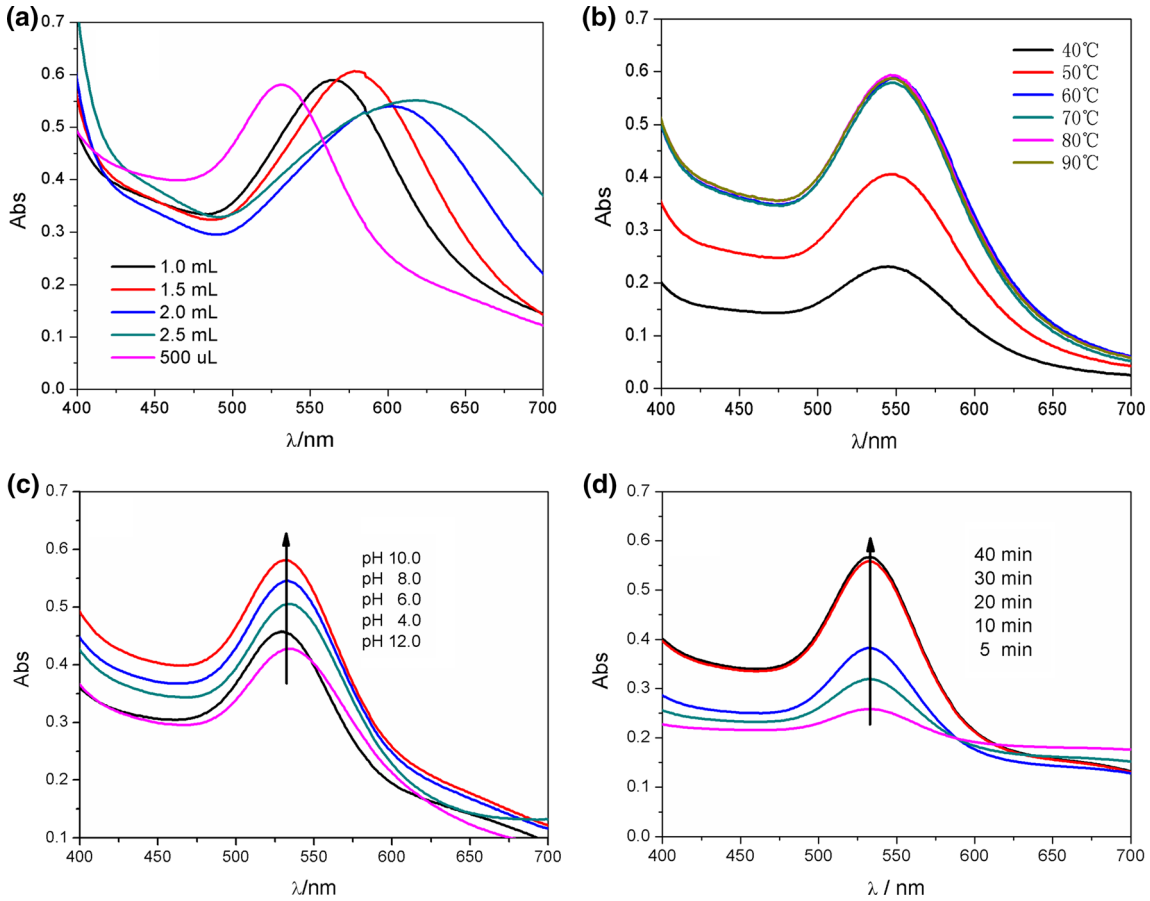

Fig. 2 UV–vis spectra of AuNPs formed at different concentrations of *G. biloba* leaf aqueous extract (**a**), reaction temperatures (**b**), pHs (**c**) and reaction durations (**d**)

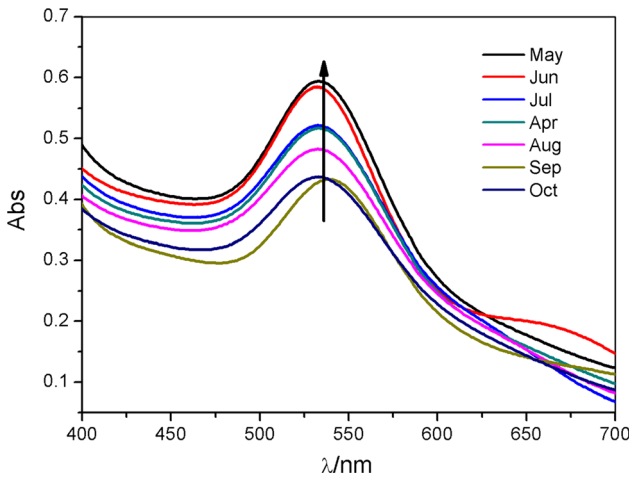

Fig. 3 UV–vis spectra of AuNPs formed by *G. biloba* leaf in seasons

larger intensity and the narrower broadness of the SPR peak of as-synthesized AuNPs were observed using the *G. biloba* leaf collected in May or June. Thus, the leaf in May was sampled for the synthesis of AuNPs in all the experiments. This is in agreement with previous studies [14, 45].

In short, in this research work, AuNPs with uniform distribution, small sizes, and good stability are biosynthesized at the optimal conditions as follow: solution pH = 10.0, reaction temperature = 60 °C, reaction duration = 30 min, *G. biloba* leaf volume concentration = 0.5 mL (sampled in May or June), and $HAuCl_4$ concentration = 0.5 mM.

Characterization of AuNPs

Typical SEM was initially used to observe the surface morphology of as-synthesized AuNPs. The particles are evidently observable owing to their size difference and uniform distribution (Fig. 4a). Unfortunately, their precise shape and size are difficult to measure by SEM micrograph, due to their size within the nano range. Therefore, the problem is settled down by the TEM experiment (Fig. 4b). It exhibits that the AuNPs are well-dispersed and revealed somewhat variable shapes but dominantly spherical in nature. Their uniform dispersion indicates that *G. biloba* macromolecules is an excellent capping agent and can produce a thin layer over the particles. The disparity size of

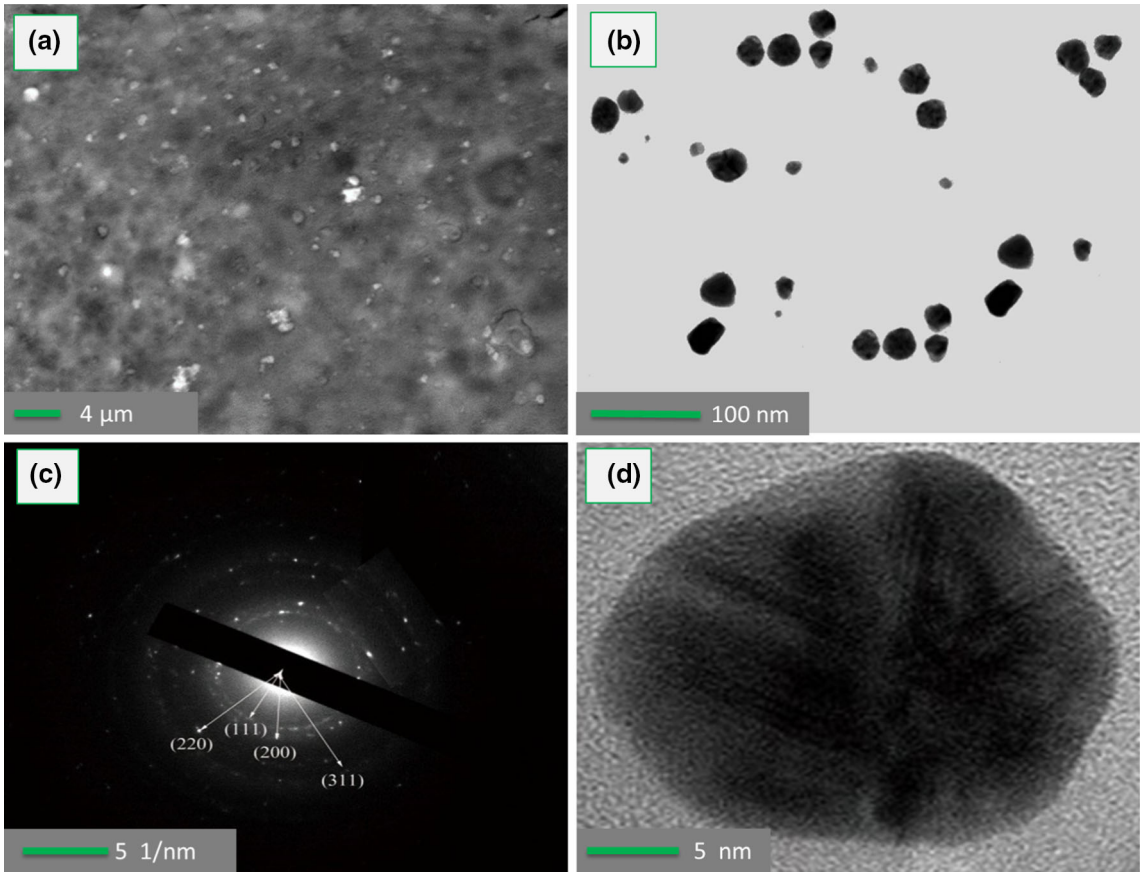

Fig. 4 **a** SEM micrograph, **b** TEM image, **c** SAED pattern, **d** HETEM image of AuNPs

the AuNPs is from 11.80 to 28.20 nm, and this distribution is further confirmed by DLS analysis. The average particle size estimated from DLS principle is found to be 18.95 ± 5.95 nm (Fig. 5a). This is obviously consistent with the TEM observation.

Figure 4c exhibits the selected area electron diffraction (SAED) pattern of the AuNPs. The ring-like diffraction pattern specifies that the particles are well crystalline. The diffraction rings could be indexed on the basis of the fcc structure of Au. Four rings arise due to reflections from (111), (200), (220) and (311) lattice planes of face-centered cubic (fcc) Au, respectively. Additionally, the clear lattice fringes having a spacing of 0.232 nm, 0.193 nm, and 0.139 nm reveals the fcc crystal lattice with (111), (200) and (220) planes, respectively. Similar SAED pattern and lattice fringes were found in AuNPs synthesized using *A. hirsutus leaves extract* [46]. The crystalline of the AuNPs was also ensured by the clear lattice fringes in the HRTEM image (Fig. 4d).

The crystalline nature of the AuNPs is further confirmed by XRD analysis (Fig. 5b). The result showed three distinct 2θ peaks at 38.16°, 44.30° and 64.58°, which indexed the planes (111), (200) and (220) planes of the Bragg's reflections of fcc structure of metallic Au respectively (JCPDS file no.-40-0784). The Debye–Scherrer's equation by measuring the width of the (111) Bragg's reflection is used to calculate the average crystallite size of particles [47]. From the Scherrer equation, about 20 nm average size is estimated. This offers reliable confirmation for the presence of AuNPs in the favor of TEM analysis and UV-absorption.

There are strong signals for Au atoms in the EDX outline of AuNPs as shown in Fig. 5c. As a result of the reduction of Au ions using *G. biloba* leaf extract, the EDX pattern evidently displays that the AuNPs are crystalline in nature. The EDX signals observed in the current study ensure the attendance of AuNPs and typically presented strong signal energy peaks at 2.12 keV (Au Mα) and 9.73 keV (Au Lα1) for Au atoms. In an earlier report [48] demonstrated the formation of separate spherical-shaped AuNPs with EDX peaks at 2.2 keV and 8.5 keV by using *Zooglea ramigera*, which is consistent with this present study. Additionally, the signal of Au ascribed to the existence of AuNPs also exposed in the EDX elemental mapping analysis (Fig. 6 red). It is also comparable to the uniformity and dispersion of particles as found in TEM and DLS.

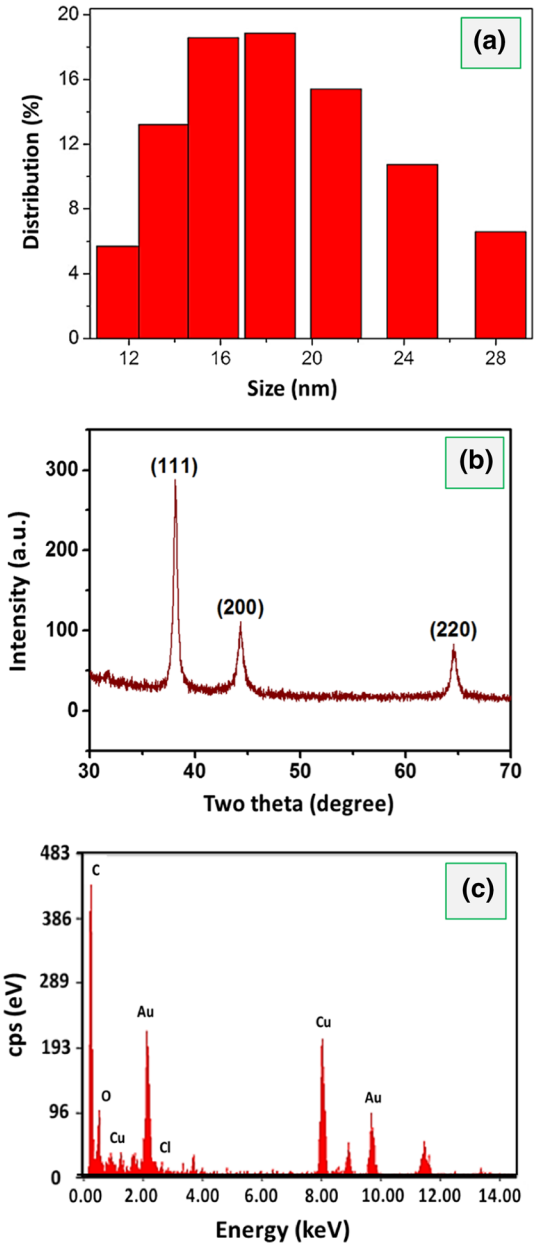

Fig. 5 **a** Particle size distributions, **b** XRD spectrum, and **c** EDX profile of AuNPs

Catalytic Degradation of Azo Dyes

The catalytic activity of the as-synthesized AuNPs is systematically investigated wherein two different azo-dyes i.e. reactive yellow 179 (RY179) and reactive yellow 145 (RY145) are successfully decolorized in an aqueous solution. Azo-dyes named after –N=N– containing synthetic dyestuffs mostly use in textile industry [49, 50]. They are highly resistant to degradation due to the presence of nitrogen molecules in their structures (Fig. 7). However, noble metal NPs has been proposed as one of the best catalysts for reducing or decolorizing azo-dyes in the presence of $NaBH_4$ [51]. Therefore, RY179 and RY145 are selected as model azo compounds for investigating the catalytic performance of the as-synthesized AuNPs in the presence of $NaBH_4$ as electron sacrificer.

The RY179 and RY145 solution shows an absorption peak at about 425 nm and 418 nm, respectively. After the addition of $NaBH_4$, and followed by magnetic stirring for 60 min, only a small amount of the solution (about 1 mL) is pipetted out. The absorbance of the solution is then taken, and it is discovered that the absorbance of RY179 and RY145 reduces by $\sim$ 22.47% and $\sim$ 30.15% respectively. This indicates a decolorization reaction. However, a fast decolorization reaction is observed in the presence of as-synthesised AuNPs catalyst. Typically, when AuNPs into the mixture containing the RY179 or RY145 and $NaBH_4$, a sudden decolorization is observed. The color of the dyes faded away and the solution becomes colorless within 30 min of reaction. Furthermore, the absorption peaks of RY179 and RY145 are measured at a time interval of 5 min as the reaction progresses. The absorbance reduces with an increase in the reaction time and finally disappeared after 30 min and 25 min for the RY179 and RY145, respectively (Fig. 7a, b).

In this context, pseudo-first-order kinetics is used to estimate the kinetics of the azo-dyes decolorization reaction. As shown in Fig. 7c, d, in the absence of AuNPs, the kinetic rate constant [ln(At/A0)] for RY179 and RY145 are estimated and found to be 0.017 and 0.0084 min^{-1} respectively. However, when AuNPs are poured into the systems, the kinetic rate constant for RY179 (Fig. 7c) and RY145 (Fig. 7d) are found to be as 0.11 min^{-1} and 0.088 min^{-1}, respectively. The results show that the AuNPs catalyst enhances the decoloration reactions of the azo-dyes for about 10 times.

Based on the above result, AuNPs performed as an electron relay that occurs the interaction between the $NaBH_4$ and azo-dyes and much faster and effectively. The mechanism behind the reaction may be hypothesized in three steps. There are- (i) adsorption of the azo-dye molecules and BH_4^- by the surface of AuNPs, (ii) transformation of electron from BH_4^- to dye molecules through AuNPs, and (iii) the generation of hydrogenated azo group, resulting in the decoloration of dyes [51]. Accordingly, the reaction mechanism of decoloration of RY179 and RY145 by $NaBH_4$ in the presence of AuNPs was drawn in Scheme 2.

Fluorescent Sensing Cr(VI)

The metal ions detection has recently received considerable attention due to the potential harm caused by various metal ions. In addition, noble metal NPs have been proved to be good catalysts for probing detection of metal ions in

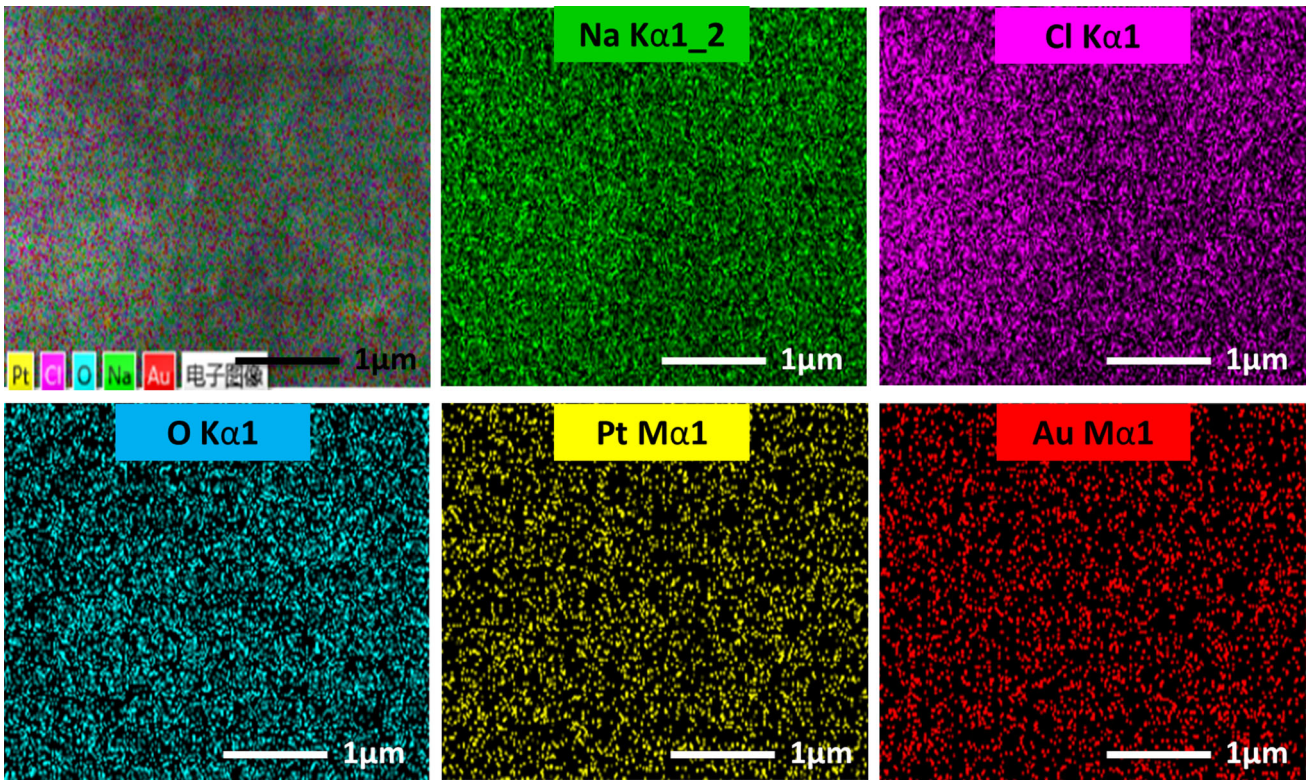

Fig. 6 SEM deployed EDX mapping of AuNPs

aqueous [52, 53]. This is due to their good catalytic and electronic properties that enable high electron conductivity. To find out the specificity of the probe, we experimented if the Cr(VI) probe detection interfered with other transition heavy metal ions. Hence, we tried nine metals namely; Hg(II), Bi(III), Pb(II), Cu (II), As (III), Co (II), Ni(II), Sb (III) and Cr(VI), as metal ions of interest. These are forbidden heavy metals in effluents of the textile companies [54]. They are used for investigating AuNPs sensitivity and selectivity towards Cr(VI). The emission spectrum of the as-synthesized AuNPs displayed an emission around a wavelength of 445 nm, and upon excitation, it shows a peak at 325 nm.

As shown in Fig. 8a fluorescence enhancement is observed in the case of Cr(VI) when compared to other metal ions. In short, it is only Cr(VI) that interacts with the intended probe while other eight metal ions make the fluorescence quenched (Fig. 8b). Fluorescence quenching is a frequently observed phenomenon when fluorophores are appended onto AuNPs [55, 56]. However, the enhancement in fluorescence by AuNPs is due to the reflected far-field radiation (Scheme 3) from the fluorophore back onto itself [57]. Therefore, it can be undoubtedly indicated that other metal ions have no effect on the fluorescence of the system, inferring that the designed fluorescence sensor demonstrates significant specificity only to Cr(VI).

For identifying a system containing Cr(VI), the optimum conditions are explored in order to confirm the accurate sensation of Cr(VI). The effect of pH on the relative fluorescence intensity (ΔF) of as-synthesized AuNPs is inspected in the different pH ranging from 7.0 to 13.0 (Fig. 9a). It is discovered that at pH 11.0 in the system of the AuNPs reacting with Cr(VI) where it is found to be the largest value of ΔF. The consequence of incubation time on the ΔF of the system is decapitated in Fig. 9b. The data revealed that the minimal increment of ΔF when AuNPs react with Cr(VI) longer than 15 min. Additionally, when the incubation time is further increased, it does not reveal any substantial transformation in the intensity, demonstrating that the reaction between Cr(VI) and AuNPs has reached an equilibrium state. Thus, the incubation time of 15 min at room temperature (25 °C) was selected as optimized reaction duration (Fig. 9b).

Thereafter, the sensitivity of the AuNPs probe for quantitative detection of Cr(VI) is tested under the as-designed optimal conditions. As shown in Fig. 10, the response of the fluorescent probe is fitted with the Stern–Volmer model. A linear connection can be found between the ΔF and the concentration of Cr(VI) over the range of 0.1–0.8 μM. Furthermore, the calibration equation which normally expresses as $(F - F0)/F = 0.99 + 0.29\ C\ (\mu M)$ has a high correlated coefficient of $R^2 = 0.995$. The limit of

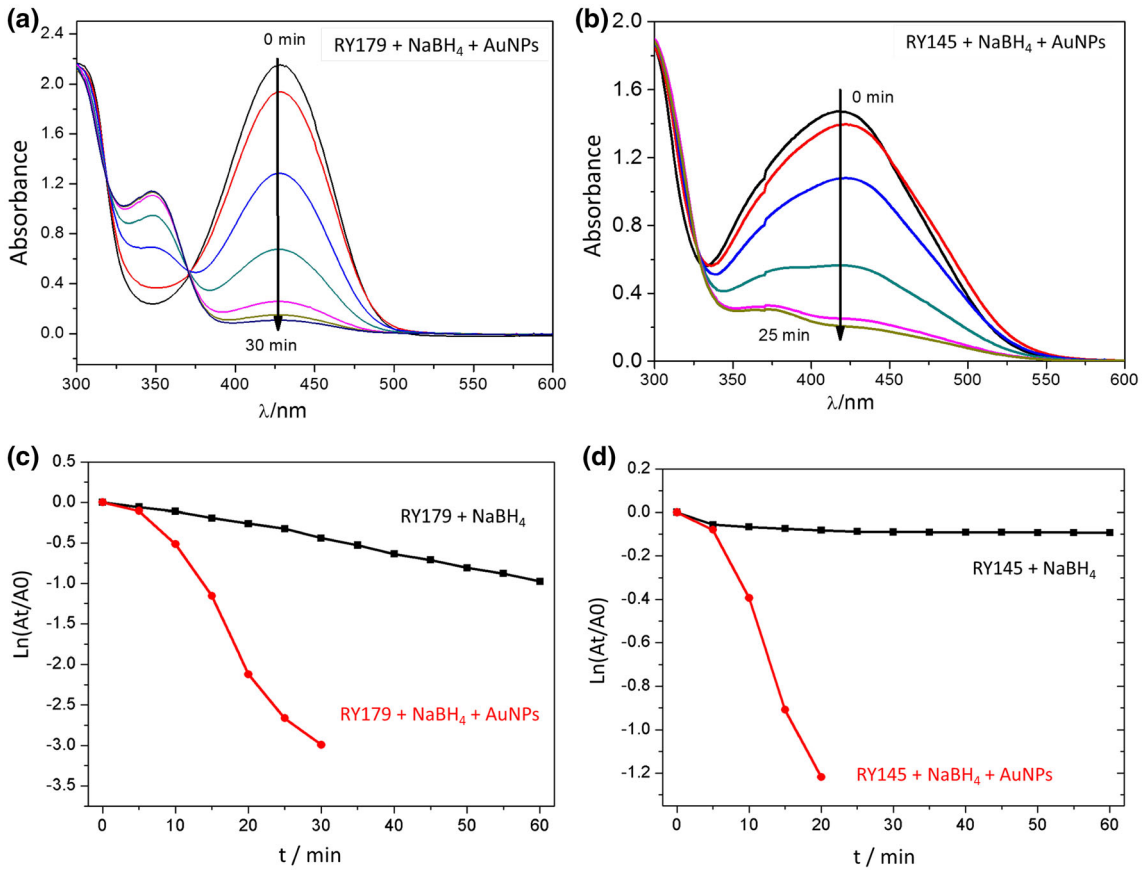

Fig. 7 The plots of absorbance against time for **a** RY179 and **b** RY145 in the presence of NaBH4 and their corresponding pseudo-first-order kinetics (**c**, **d**)

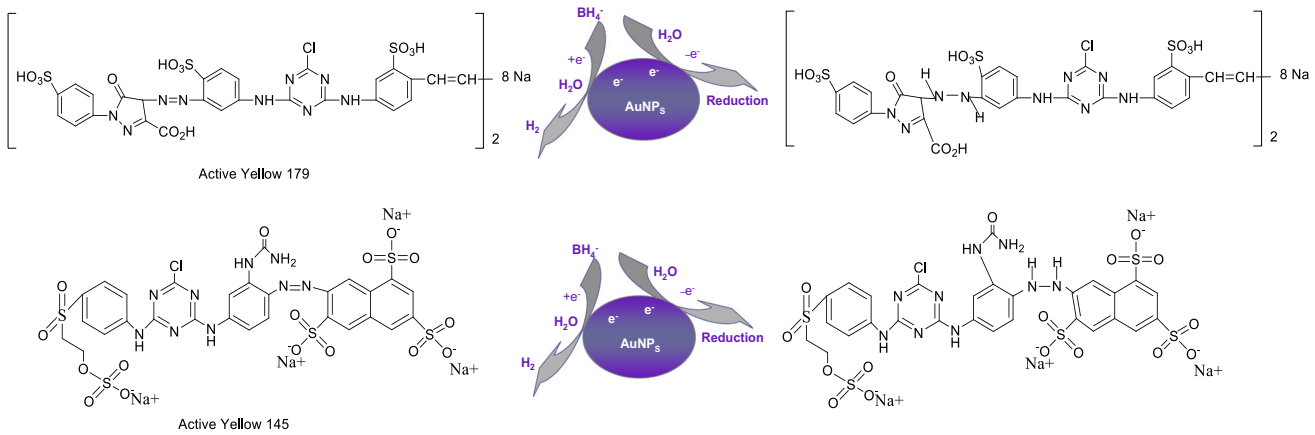

Scheme 2 The proposed decoloration mechanism of azo dyes by $NaBH_4$ in the presence of AuNPs

detection (LOD) for Cr(VI) is calculated and found to be 3.3 nM. All these results show that the as-synthesized AuNPs exhibit high sensitivity towards Cr(VI) detection in aqueous solution.

In a judgment with other fluorescence methods as shown in Table 1, these analytical parameters are comparable or somehow better than those previously reports [23–27]. According to the regulation of the World Health Organization (WHO), a concentration of Cr(VI) with threshold limit < 1.0 μM is acceptable in drinking water [58]. This indicates that our as-synthesized AuNPs probe is sensitive enough to monitor Cr(VI) concentration in drinking water.

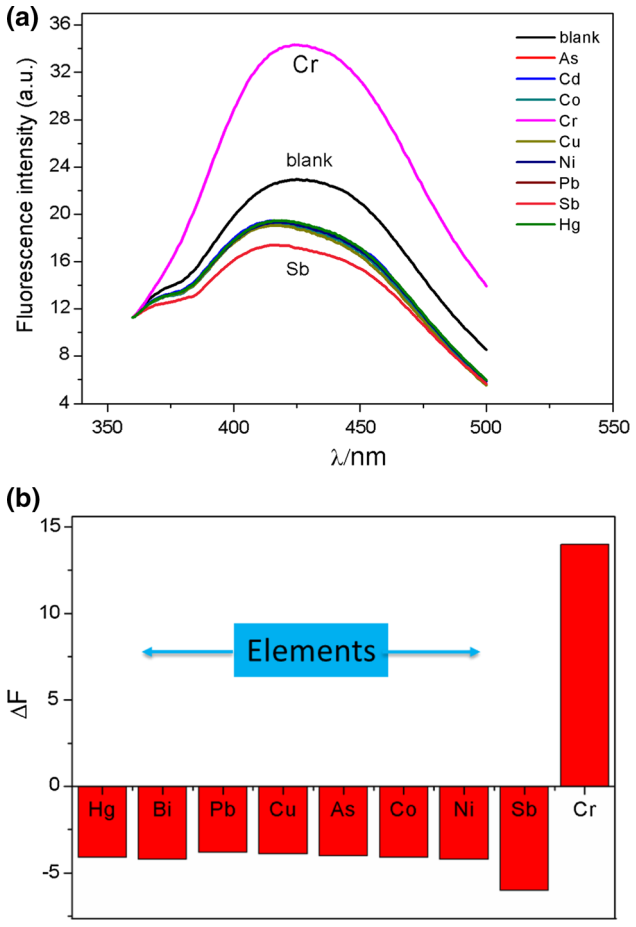

Fig. 8 Fluorescence spectra **a** and intensity histograms **b** of AuNPs in the presence of nine metal ions

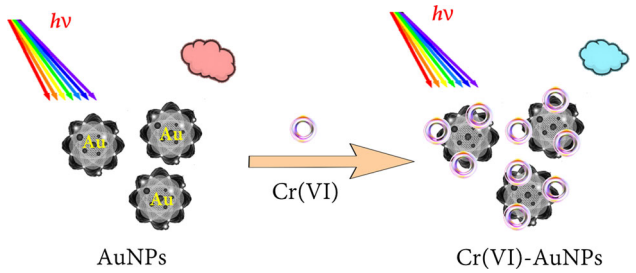

Scheme 3 Schematic illustration of the fluorescent sensing of Cr(VI) with AuNPs

Conclusions

In this work, AuNPs are synthesized via the biosynthetic method by using *G. biloba* leaf aqueous extract as reducing and stabilizing agents. The effects of synthesis variables like the reductant concentration, mixing ratio of $HAuCl_4$ to *G. biloba* leaf aqueous extract and reaction time on the formation of AuNPs with small size and uniform distribution are investigated. Synthesis is found to be effective with 0.5 mL *G. biloba* leaf aqueous extract diluted to

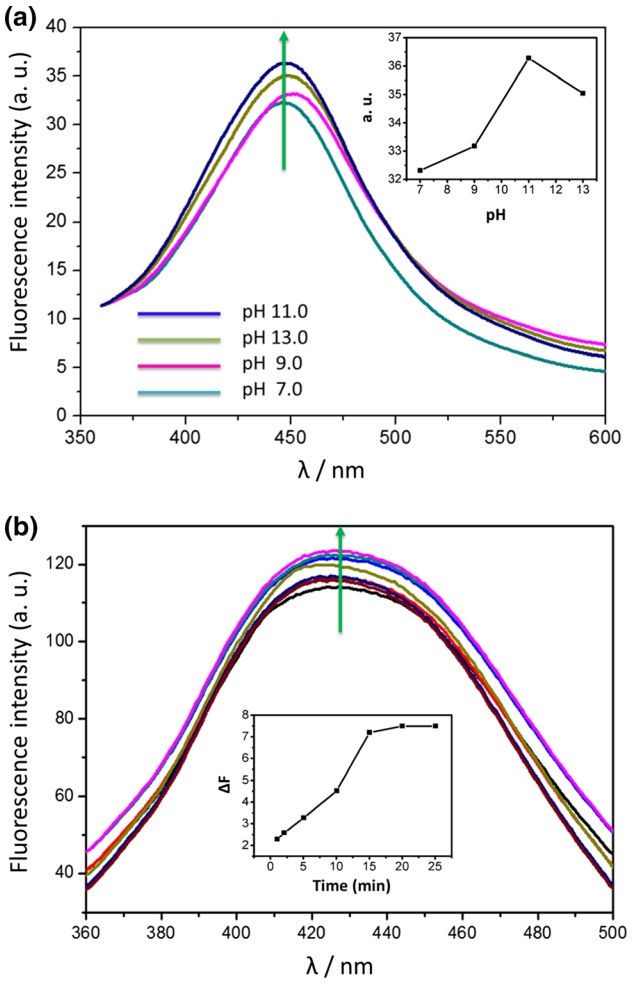

Fig. 9 **a** Fluorescence spectra of AuNPs at different pHs. Inset: the fluorescence intensities against pH values; **b** fluorescence spectra at different durations. Inset: the intensities against reaction time

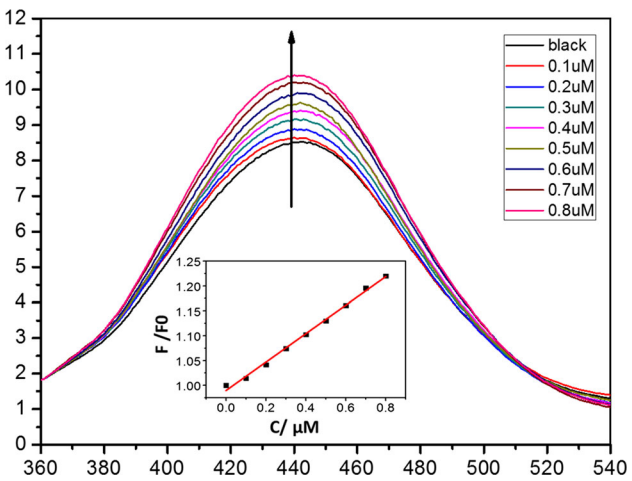

Fig. 10 Fluorescence intensity plotted against the Cr(VI) concentration. Inset: Fluorescence spectra of AuNPs by adding Cr(VI) concentrations

Table 1 Comparison of different fluorescent probes for the determination of Cr(VI)

Detection method	Reagents	Linear range (μM)	LOD (nM)	Refs.
Fluorescent spectrometry	As-synthesizedAuNPs	0.10–0.80	3.30	This work
Fluorescent spectrometry	Graphene quantum dots	0.05–500	3.70	[23]
Electrochemical technique	Ti/TiO_2 nanotube/Au electrode	0.10–105	0.03	[24]
Spectrofluorimetry	Rhodamine B hydrazide	0.05–2.00	5.50	[25]
Electrochemical technique	Au–Ag–Pt three material electrodes	2.00–200	0.90	[26]
Graphite furnace atomic absorption spectrometry	β-Cyclodextrin-crosslinked polymer	0.038–3.10	0.06	[27]

5.0 mL solution against 0.5 mM $HAuCl_4$, solution pH of 10.0, reaction temperature of 60 °C and reaction duration of 30 min. It has been confirmed that the uniformly dispersed spherical shape AuNPs can be synthesized in a green way by using *G. biloba* leaf aqueous extract. The AuNPs exhibit appreciable catalytic activity for the decolorization of azo-dyes in the presence of sodium borohydride as electron sacrificer. On the other hand, Cr(VI) makes the fluorescence enhancement of AuNPs which is sensitive enough to monitor Cr(VI) concentration in drinking water. This work is expected to spur further work on the use of biosynthesized AuNPs for sensors and water remediation applications.

Acknowledgements The authors thank the kind support of this work from the Innovation Platform Projects of Wuhan Textile University (183052).

References

1. S. Ahmed, S. Ikram, and S. S. Yudha (2016). *J. Photochem. Photobiol. B Biol.* **161**, 141.
2. T. Ahmad, M. A. Bustam, M. Irfan, M. Moniruzzaman, H. M. A. Asghar, and S. Bhattacharjee (2018). *J. Mol. Struct.* **1159**, 167.
3. M. Teimouri, F. Khosravi-Nejad, F. Attar, A. A. Saboury, I. Kostova, G. Benelli, and M. Falahati (2018). *J. Clean. Prod.* **184**, 740.
4. J. Lee, H. Y. Kim, H. Zhou, S. Hwang, K. Koh, D.-W. Han, and J. Lee (2011). *J. Mater. Chem.* **21**, 13316.
5. R. Mohammadinejad, S. Karimi, S. Iravani, and R. S. Varma (2016). *Green Chem.* **18**, 20.
6. F. Mares-Briones and G. Rosas (2017). *J. Clust. Sci.* **28**, 1995.
7. N. Saha and S. D. Gupta (2016). *J. Clust. Sci.* **27**, 1419.
8. K. B. Narayanan and N. Sakthivel (2008). *Mater. Lett.* **62**, 4588.
9. J. Huang, Q. Li, D. Sun, Y. Lu, Y. Su, X. Yang, H. Wang, Y. Wang, W. Shao, and N. He (2007). *Nanotechnology* **18**, 105104.
10. M. Guo, W. Li, F. Yang, and H. Liu (2015). *Spectrochim. Acta A Mol. Biomol. Spectrosc.* **142**, 73.
11. S. P. Chandran, M. Chaudhary, R. Pasricha, A. Ahmad, and M. Sastry (2006). *Biotechnol. Prog.* **22**, 577.
12. E. Pereira, L. Barros, M. Dueñas, A. L. Antonio, C. Santos-Buelga, and I. C. Ferreira (2015). *Ind. Crops Prod.* **74**, 144.
13. L. Zhang, S. Guo, M. Wang, and L. He (2015). *Int. J. Biol. Macromol.* **80**, 644.
14. T. A. van Beek and P. Montoro (2009). *J. Chromatogr. A* **1216**, 2002.
15. Y. Y. Ren, H. Yang, T. Wang, and C. Wang (2016). *Phys. Lett. A* **380**, 3773.
16. M. Nasrollahzadeh and S. M. Sajadi (2015). *J. Colloid Interface Sci.* **457**, 141.
17. S. Gurunathan, J. W. Han, J. H. Park, V. Eppakayala, and J. H. Kim (2014). *Int. J. Nanomed.* **9**, 363.
18. J. L. Zha, C. F. Dong, X. J. Wang, X. L. Zhang, X. H. Xiao, and X. Z. Yang (2017). *Optik* **144**, 511.
19. Y. Ma, Y. Chen, J. Liu, Y. Han, S. Ma, and X. Chen (2018). *Talanta* **185**, 249.
20. H. Wang and C. Na (2014). *ACS Appl. Mater. Interfaces* **6**, 20309.
21. D. Dong, X. Zhao, X. Hua, J. Liu, and M. Gao (2009). *J. Hazard. Mater* **162**, 1261.
22. L. Zhang, C. Xu, and B. Li (2009). *Microchim. Acta* **166**, 61.
23. S. Huang, H. Qiu, F. Zhu, S. Lu, and Q. Xiao (2015). *Microchim. Acta* **182**, 1723.
24. W. Jin, G. Wu, and A. Chen (2014). *Analyst* **139**, 235.
25. Y. Xiang, L. Mei, N. Li, and A. Tong (2007). *Anal. Chim. Acta* **581**, 132.
26. D. Li, J. Li, X. Jia, Y. Xia, X. Zhang, and E. Wang (2013). *Anal. Chim. Acta* **804**, 98.
27. Y. Gu and X. Zhu (2011). *Microchim. Acta* **173**, 433.
28. V. Arancibia, M. Valderrama, K. Silva, and T. Tapia (2003). *J. Chromatogr. B* **785**, 303.
29. S. Cathum, C. Brown, and W. Wong (2002). *Anal. Bioanal. Chem.* **373**, 103.
30. K. Hunger *Industrial dyes: chemistry, properties, applications* (Wiley, Hoboken, 2007).
31. R. Kant (2012). *Nat. Sci.* **4**, 22.
32. H. Li, Q. Chen, S. Li, W. Yao, L. Li, X. Shi, L. Wang, V. Castranova, V. Vallyathan, and E. Ernst (2001). *Ann. Occup. Hyg.* **45**, 505.
33. S. Arunkumar and M. Alagiri (2017). *J. Clust. Sci.* **28**, 2635.
34. I. Safarik, L. Ptackova, and M. Safarikova (2002). *Eur. Cells Mater.* **3**, 52.
35. A. G. Assefa, A. A. Mesfin, M. L. Akele, A. K. Alemu, B. R. Gangapuram, V. Guttena, and M. Alle (2017). *J. Clust. Sci.* **28**, 917.
36. L. Bo, Y. Zhang, X. Quan, and B. Zhao (2008). *J. Hazard. Mater.* **153**, 1201.
37. A. K. Chakraborty, S. Ganguli, and M. A. Kebede (2012). *J. Clust. Sci.* **23**, 437.
38. T. A. van Beek (2002). *J. Chromatogr. A* **967**, 21.
39. S. Mahmud, M. Z. Sultana, M. N. Pervez, M. A. Habib, and H.-H. Liu (2017). *Fibers* **5**, 35.
40. Z. Shervani and Y. Yamamoto (2011). *Mater. Lett.* **65**, 92.
41. S. Mahmud, N. Pervez, M. Z. Sultana, A. Habib, and L. Hui-Hong (2017). *Orient. J. Chem.* **33**, 2198.
42. B. Yang, J. Chou, X. Q. Dong, C. T. Qu, Q. S. Yu, K. J. Lee, and N. Harvey (2017). *J. Phys. Chem. C* **121**, 8961.

43. N. Y. Polyakova, A. Y. Polyakov, I. V. Sukhorukova, D. V. Shtansky, and A. V. Grigorieva (2017). *Gold Bull.* **50**, 131.
44. S. Mahmud, M. N. Pervez, M. A. Habib, M. Z. Sultana, and H.-H. Liu (2018). *Asian J. Chem.* **30**, 116.
45. S. Y. Cheng, F. Xu, and Y. Wang (2009). *J. Med. Plants Res.* **3**, 1248.
46. I. Vijayashree, P. Niranjana, G. Prabhu, V. Sureshbabu, and J. Manjanna (2017). *J. Clust. Sci.* **28**, 133.
47. S. H. Koli, B. V. Mohite, H. P. Borase, and S. V. Patil (2017). *J. Clust. Sci.* **28**, 2719.
48. N. Srivastava and M. Mukhopadhyay (2015). *J. Clust. Sci.* **26**, 675.
49. V. Thangaraj, S. Mahmud, W. Li, F. Yang, and H. H. Liu (2018). *IET Nanobiotechnol.* **12**, 47.
50. L. S. Duan, M. Li, and H. H. Liu (2015). *IET Nanobiotechnol.* **9**, 349.
51. Y. Li, G. Li, W. Li, F. Yang, and H. H. Liu (2015). *Nano*. https://doi.org/10.1142/S1793292015501088.
52. J. Song, Q. Ma, S. Zhang, Y. Guo, and C. Dong (2016). *J. Clust. Sci.* **27**, 1203.
53. B. R. Gangapuram, R. Bandi, R. Dadigala, G. M. Kotu, and V. Guttena (2017). *J. Clust. Sci.* **28**, 2873.
54. C. Rongqi (2002). *Dye. Finish.* **5**, 26–31.
55. Y. Li, G. Li, K. L. Lei, M. Li, and H. H. Liu (2016). *Chin. J. Anal. Chem.* **44**, 773.
56. G. Li, Y. L. Sun, and H. H. Liu (2018). *J. Clust. Sci.* **29**, 177.
57. E. G. Matveeva, Z. Gryczynski, J. Malicka, J. Lukomska, S. Makowiec, K. W. Berndt, J. R. Lakowicz, and I. Gryczynski (2005). *Anal. Biochem.* **344**, 161.
58. G. WHO (World Health Organization, 2011) vol. 216, pp. 303.